Health Monitoring of LSF Structure via Novel TTFD Approach

Hamid Reza VOSOUGHIFAR[*1] and Seyed Kazem SADAT SHOKOUHI[1]

[1]Department of Civil Engineering, Islamic Azad University, South Tehran Branch, Tehran, Iran, PH +98(21)882-06714; FAX +98(21)882-06718; email: vosoughifar@azad.ac.ir, shokouhi.eng@gmail.com

Abstract. Lightweight Steel Framing (LSF) system has been proposed as an economic system and earthquake-resistant. Structural Health Monitoring (SHM) is as conservator for structure and monitor structure situation from stress and strain between different elements as continues. In this paper, a LSF building was modeled using Finite Element Method (FEM) which Modal and Time-history Analyses were utilized considering the effects of Near-field and Far-field earthquakes. Furthermore, three various Optimal Sensor Placement (OSP) algorithms were used and Genetic Algorithm (GA) was selected to act as the solution of the optimization formulation in the selection of the best sensor placement according to structural dynamic response of the LSF system. Results show that with a proper OSP method for SHM can detect weak points of structure in different parts and then can retrofit mentioned points.

Keywords: Lightweight Steel Framing (LSF), Finite Element Method (FEM), Optimal Sensor Placement (OSP), Genetic Algorithm (GA), Near-field and far-field earthquakes.

1. Introduction

Lightweight Steel Framing (LSF) systems have been used for low and medium rise residential, industrial and commercial building construction. The advantages of cold-formed steel, such as being dimensionally stable, noncombustible, termite and borer proof, durable, lightweight and 100% recyclable, are probably important reasons for this increase in use.

In recent years, there have been many experimental and analytical studies on Cold-Formed Steel (CFS) profiles, members and framing systems. Xu and Tangorra [1] presented the experimental results of a study carried out at the University of Waterloo on vibration characteristics of cold formed steel supported lightweight residential floor systems. Al-Kharat and Rogers [2] presented an experimental overview of the inelastic performance of sixteen 2.44 m × 2.44 m cold-formed steel strap braced walls that were not designed following a strict capacity based design. Using monotonic and reversed cyclic loading protocols, they showed that if capacity design principles are not considered, it is possible for the performance of the walls to be affected by the hold down detail, which in many cases did not allow the test specimens to reach or maintain a yield capacity and severely diminished the overall system ductility. Dan Dubina [3] summarizes the research activities carried out in the last few years at the Politehnica University of Timisoara, under the coordination of the author, with the aim to evaluate the performance and to characterize for design purpose the specific features of light steel framed structures. Monotonic and cyclic tests on full-scale shear panels, tests on connection details, and in situ ambient vibration tests on a house under construction are reviewed and concluded in this paper. Moghimi and Ronagh [4] studied on the performance of different light-gauge cold-formed steel strap-braced stud wall arrangements subjected to

License: http://creativecommons.org/licenses/by/3.0/

cyclic on a total of twenty full-scale 2.4 m × 2.4 m specimens and presented the techniques to improve their behavior. Steel is light in weight, but it exhibits high strength, excellent seismic performance, and recyclability, which meet the demands of continuous development in civil engineering [5].

To detect damage throughout the whole structure, especially some large, complicated structures, the vibration-based identification techniques show great promise because they allow for quick and efficient damage detection at a relatively low cost after a severe loading event such as an earthquake or hurricane [5]. Many methods for diagnosing damage have been developed based on vibration detection, e.g., sensitivity analysis methods [6], regularization methods [7], model-updating methods [8-9], artificial neural networks [10-11], wavelet transform approaches [12-13], and the damage location vector [14-15]. The damage parameters should reflect the damage location and damage extent in specific areas of single components. For a beam or column element, it may be appropriate to choose multiple damage indicators to represent damage in various sites, such as beam-column joints and the central of elements. Location of sensors is one of the most important factors in a monitoring network and it needs to be optimized to maximize system performance and reduce the cost of the system [5]. Hemez and Farhat [16] extended the effective independence method in an algorithm where sensor placement was achieved in terms of the strain energy contribution of the structure. Miller [17] computed a Gaussian quadrature formula using the functional gain as a weight function, and thought that the nodes of the quadrature formula gave the optimal locations for sensors. Hiramoto et al. [18] used the explicit solution of the algebraic Riccati equation to determine the optimal sensor/actuator placement for active vibration control. Wouwer et al. [19] presented an optimality criterion for the selection of optimal sensor locations; the criterion was based on a measure of independence of the sensor responses. Worden and Burrows [20] used a number of different methods to determine an optimal sensor distribution based on the curvature data. Also, Cobb and Liebst [21] and Shi et al. [22] have reported the Optimal Sensor Placement (OSP) for the purpose of detecting structural damage. In recent years, Cruz et al. [23] and Yi et al. [24] performed new researchers about OSP for two different structures. In this research, a LSF building was modeled using Finite Element Method (FEM) which Modal and Time-history Analyses were utilized considering the effects of Near-field and Far-field earthquakes. Furthermore, three various OSP methods were used and Genetic Algorithm (GA) was selected to act as the solution of the optimization formulation in the selection of the best sensor placement according to structural dynamic response of the steel building.

2. Structural Modeling Description

In this paper, a 4-stories LSF structure was chosen for three-dimensional analysis with an irregular plan. A 3D view of the FE structural models is shown in Figure 1.

This building considered has the various plans and the LRFD design method was utilized in the designing procedure based on AISI standard [37]. It was located in the high damage risk zone of the Tehran city. The main frame of the wall panels were made of cold-formed steel elements, top and bottom tracks were U204/2.0 (U shape with 204*100 and Th. 2.0 mm dimension), while studs were C200/2.0 profiles, fixed at each end to tracks with self-drilling self-taping screws. In this building using cement board sheet as cladding the sheets were placed in a horizontal position with a useful width of 1200 mm. Cement boards sheet was fixed to the wall frame using special self-tapping screws. The number of screws being determined to avoid failure at strap end fixings and facilitate yielding. 10 mm OSB panels (1200 × 2440 mm) were placed in similar way as the gypsum panels in internal spaces of building, only on the ‘external’ side of the panel and fixed to the frame using bugle head self-

drilling screws of d = 4.2 mm diameter at 1 mm intervals. It should be noted that different experimental tests were conducted on the cold-formed profiles in the Mechanics Laboratory of Sharif University of Technology (see Figure 2) which Table 1 presents the material properties according to the mentioned laboratory results.

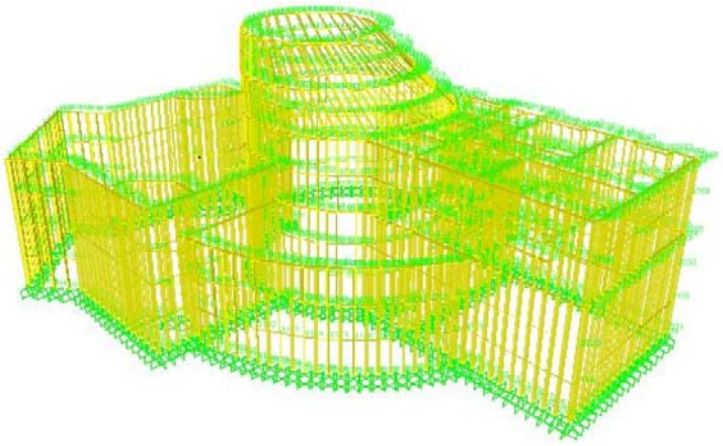

Figure 1 3D view of the FE structural model

Figure 2 The performed different laboratory tests on the cold-formed profiles

Table 1 The material properties data

Yield strength (f_y-kg/cm^2)	Ultimate tensile strength (f_u-kg/cm^2)	E (Cold Formed-kg/cm^2)	ϑ (Cold Formed)	G (Cold Formed - kg/cm^2)
3510	4560	2.074×10^6	0.3	7.977×10^5

3. Analysis Procedure

3.1. Time-history Analysis

Six sets of recorded earthquake ground motions including near-field and far-field seismic records were selected from the Pacific Earthquake Engineering Research database [25] for the purpose of dynamic analysis. Time-history analyses were conducted using a FE software to evaluate dynamic response of presented structural system. Dynamic analyses using 6 scaled earthquake ground motions were performed for each model. Seismic responses are obtained in x, y and z directions. The time histories obtained are maximum base shear, moment and lateral displacements in the *x* and *y* directions. It should be noted that due to model accounts directly for effects of material elastic response, the resulting internal forces are reasonable approximations of those expected during the design earthquake. The evidences in Tables 2 and 3 have been attained from dynamic analyses of the 3-story LSF building considering near-field and far-field earthquakes.

Table 2 Maximum results of time-history analyses for a LSF building using near-field earthquakes

Earthquake	Design base shear (Kgf) in the x-direction	Design base shear (Kgf) in the y-direction	Design base moment (Kgf-cm) in the x-direction	Design base moment (Kgf-cm) in the y-direction	Top-story displacement in x-direction (cm)	Top-story displacement in y-direction (cm)
Chi-Chi (1999)	3093	2829	763118.67	706986.63	9.13	8.26
Chi-Chi (1999)	2924	2653	731138.96	665514.06	8.72	7.89
Northridge (1994)	2740	2316	685628.09	611874.69	8.14	7.34

Table 3 Maximum results of time-history analyses for a LSF building using far-field earthquakes

Earthquake	Design base shear (Kgf) in the x-direction	Design base shear (Kgf) in the y-direction	Design base moment (Kgf-cm) in the x-direction	Design base moment (Kgf-cm) in the y-direction	Top-story displacement in x-direction (cm)	Top-story displacement in y-direction (cm)
Chi-Chi (1999)	3038	2631	731108.67	696846.63	8.41	7.76
Chi-Chi (1999)	2245	2474	711308.96	655214.06	8.11	7.29
Northridge (1994)	2408	2177	656208.09	601174.69	7.63	7.04

3.3 Modal Analysis (MA)

Natural time periods or natural frequencies are the important characteristics of a structure. It can be used to analyze the results obtained by dynamic analysis. To evaluate natural frequencies, modal analysis of LSF building has been carried out. Table 4 shows the first three natural time periods and maximum modal responses of the proposed FE model respectively. Figure 3 illustrates also the effective mode shapes of braced structure. According to Iranian seismic code [34] the mode shapes with periods more than 0.4 seconds or the modes that have participation contribution more than 90 present of mass are mentioned ($T > 0.4$ sec = $F < 2.5$ cycles/sec). Hence in this research the first 3 modes were considered as efficient modes.

Table 4 Modal results: periods and maximum displacement in the X, Y and Z directions

Mode no.	Period (sec)	Max displacement (X-cm)	Max displacement (Y-cm)	Max displacement (Z-cm)
1	0.63	16.28	14.74	12.82
2	0.52	14.73	12.19	11.65
3	0.49	11.01	10.44	9.77
4	033	8.23	8.06	7.91
5	0.31	7.54	7.37	7.16

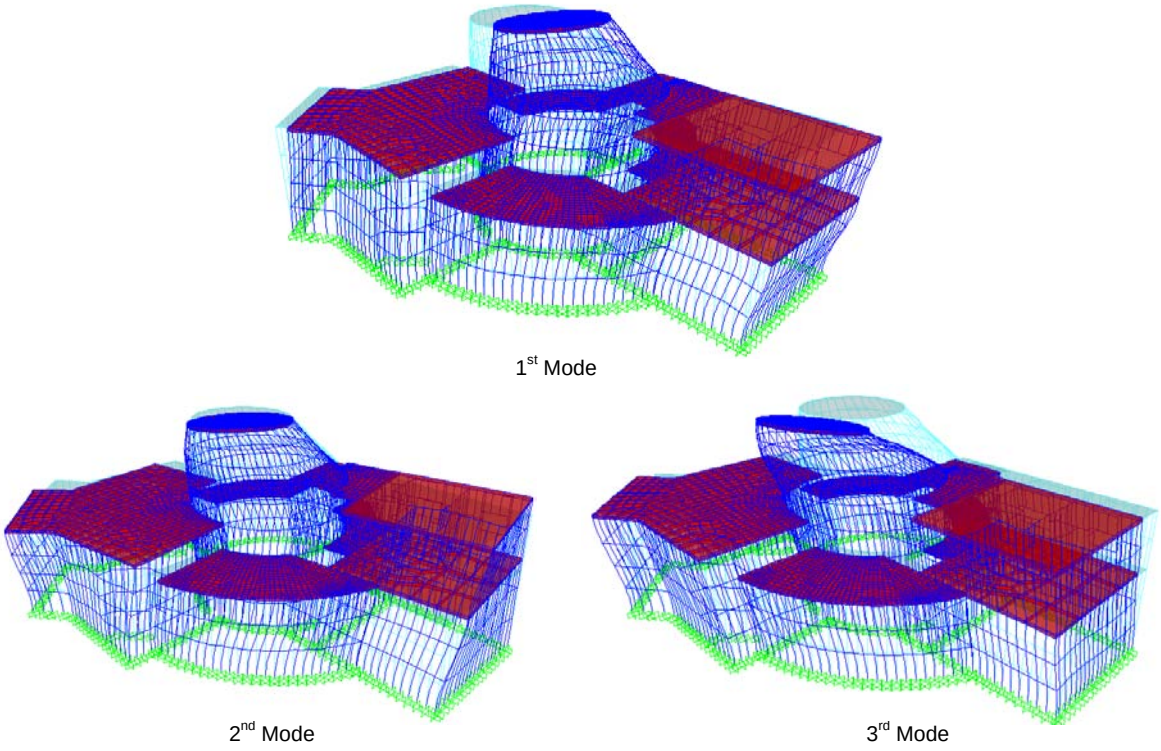

Figure 3 The effective mode shapes of LSF structure

4. Genetic Algorithm

To find the optimal solution of the objective function given in the previous section, genetic algorithms were used. Genetic algorithm is well known due to its simplicity and robustness in the solution of complex problems, and these characteristics fit well to the problem described here [26]. The length of an individual chromosome depends on the number of sensors and all integer numbers in a chromosome should be unique. To place the sensors simultaneously, a genetic algorithm is an effective method.

GAs have been widely used in sensor placement type problems [27]. They have been used to search for the optimal locations of actuators in active vibration control [28]. Another type of problem where GAs have been successfully utilized is the placement of vibration isolators to reduce the transmissibility of undesirable vibrations to an optical laboratory table [29]. However, these methods often produce some invalid strings in the evolution process.

GA has been proved to be a powerful tool to OSP, but it also has some faults that need to be improved. For example, one sensor location may be placed where two or more sensors or sensor numbers are not equal to a certain number [30]. A good surveillance system must detect the aftermath of a contaminant spill as soon as possible with maximum reliability. Earlier detection gives more time for the system managers to react. Thus an objective of the optimization is to maximize the detection time that can be defined in an average sense and an objective function.

In this optimization method, information about a problem, such as variable parameters, is coded into a genetic string known as a chromosome (individual). Each of these chromosomes has an associated fitness value, which is usually determined by the objective function to be maximized or minimized. Each chromosome contains substrings known as genes, which contribute in different ways to the fitness of the chromosome. It should be noted that an essential characteristic of a GA is the coding of the variables that describe the problem. A binary coding method can be used. The method is to transform the variables to a binary string of specific length. Also, Crossover is the operator that produces new individuals (offspring) by exchanging some bits of a couple of randomly selected individuals (parents). Furthermore, Mutation operates on a single individual with a small probability. With this operation, one or more bits are chosen at random from the individual and changed into a different symbol [31].

5. Sensor Placement Optimization Procedure

Numerous techniques have been advanced for the OSP problem and are widely reported in this literature. These have been developed using a number of approaches and criteria, some based on intuitive placement or heuristic approaches, others employing systematic optimization methods. The sensor placement optimization can be generalized as “given a set of n candidate locations, find the subset of m locations, where $m \leq n$, which may provide the best possible performance” [24].

In the case under investigation the fitness function is a weighting function that measures the quality and the performance of a specific sensor location design. This function is maximized by the GA system in the process of evolutionary optimization. As known, the measured mode shape vectors in the SHM have to be as possible linearly independent, which is a basic requirement to distinguish, measured or identified modes. Hence, three different OSP algorithms were utilized which include Modal Assurance Criterion (MAC), Extended MAC (EMAC) and Transformed Time-history to Frequency Domain (TTFD).

5.1 MAC Algorithm

The simple way to check linear dependence of mode shapes is to calculate the MAC [32]. It is equivalent to maximize the angles formed by unit mode shape vectors, or to minimize the dot product between them, which is the same as the MAC. The MAC without mass weighting is just to compare the direction of two vectors. When two vectors lie in the same direction or near, the MAC value or the correlation coefficient is one or approximate one. Small maximum off-diagonal term indicates less correlation between corresponding mode shape vectors, and renders the mode shapes discriminable from each other. The fitness function presented in this section is constructed by the MAC, the biggest value in all the off-diagonal elements in the MAC matrix. The reason for the selection of this kind of fitness function is that the MAC matrix will be diagonal for an optimal sensor placement strategy so the size of the off-diagonal elements can be taken as an indication of the fitness. The MAC can be defined as Equation (1), which measures the correlation between mode shapes:

$$MAC_{ij} = \frac{(\Phi_i{}^T \Phi_j)^2}{(\Phi_i{}^T \Phi_i)(\Phi_j{}^T \Phi_j)} \quad (1)$$

where, Φ_i and Φ_j represent the ith and jth column vectors in matrix Φ, respectively, and the superscript T denotes the transpose of the vector. In this formulation, the values of the MAC range between 0 and 1, where zero indicates that there is little or no correlation between the off-diagonal element MAC_{ij} $(i \neq j)$ and one means that there is a high degree of similarity between the modal vectors [32].

Then the MAC fitness function is given as Equation (2):

$$f = 1 - \max\left(abs\left(MAC_{ij}\right)\right) \quad (i \neq j) \quad (2)$$

For this attempt, the size of the searching space is the number of nodes on the FE model excluding the constrained nodes and the vibration nodes of the selected modes. The MAC algorithm achieves this objective as follows. First, an intuition sensor set (much less than the required number of sensors) is selected based on experience and requirements of structural topology for visualization of mode shapes. Second, it adds other available candidate sensors one by one, and selects one that minimizes the maximum off-diagonal element of the MAC matrix at each step. Third, the MAC repeats the second step by adding one sensor at a time until a required number of sensors are selected. When performing the OSP method via GA technique, certain parameters are required such as; constraints, Fitness function, population, generation, crossover method, mutation rate etc. Each of these runs started with a random initial population that was uniformly distributed within the same range.

The locations selected for the 2 accelerometers needed to be installed. It should be noticed that due to the nature of the GA method, the results are usually dependent on the randomly generated initial conditions, which means the algorithm may converge to a different result in the parameter space. These values are very close to the optimal value.

5.2 EMAC Algorithm

To overcome the contra-decreasing problem of the original MAC algorithm, a forward-backward combinational extension is developed as follows by Dongsheng [33]. An EMAC algorithm proposed to overcome the disadvantages of traditional MAC algorithm with the introduction of a forward-backward combinational approach. First, an intuition sensor set, U_0 (including, to say, a number of sensors, s_0) is chosen. Then, one sensor is added to this initial set until a preset number of sensors, which is somewhat larger than the number of sensors as required, for instance, ten percent more than required ($1.1s_0$), is reached. This is the same forward sequential MAC procedure. The extension differs from the original forward approach in the stopping criterion. The EMAC algorithm is continued to obtain a sensor set, U_1, consisting a certain number of sensors (to say, s_1, $s_1 \leq 1.1s_0$) larger than the required one s_0 where the original MAC stops.

Secondly, one sensor at each step is excluded from the sensor set U_1 until the required number of sensors s_0 is reached. This is the backward sequential MAC approach, the essential extension to the forward one. Therefore, two function curves are established. One is the curve of the maximum off-diagonal term with respect to the number of sensors increasing from s_0 to s_1 be obtained in the first stage, and the other is the curve of the maximum off-diagonal term with respect to the number of sensors decreasing from s_1 to s_0 found in the second stage. Both curves are compared and the one with a smaller value at the point s_0 is selected. Which curve is to be selected, depends on the abilities of the forward and backward

approaches to minimize the maximum off-diagonal terms of the MAC matrix. In this manner, the maximum off-diagonal term of the MAC matrix may, in many instances, be further minimized than the traditional MAC algorithm [33].

Naturally, the forward stopping number of sensors s_1 in the first step can be varied according to the structure under consideration. The effects of various numbers s_1 of sensors on the selection set (including s sensors) of the above two step processes can be compared and the one with the smallest maximum off-diagonal term of the MAC matrix can be chosen. This can be implemented as the third step, if necessary.

As before section, 2 accelerometers needed to be installed. As explained before, the results are usually dependent on the randomly generated initial condition that means the algorithm may converge to a different result in the parameter space. These values are very close to the optimal value. Figure 4, illustrates which the best fitness values tend to a constant quicker along as the number of generations increases despite many fluctuations occurring that are caused by the genetic operators of crossover and mutation's search procedures.

There is one note about the influence of the choice of the intuition sensor set, U_0, on the final selection of sensor positions. If a newly added sensor conflicts with one or several of the original intuition set, the intuition set maybe reformed if the exclusion of certain sensor from the original intuition set U_0 is not considered to be much detrimental to the mode shape visualization. Afterwards, the two steps can be recomputed. The optimal locations for the MAC and EMAC algorithms are illustrated in Table 5.

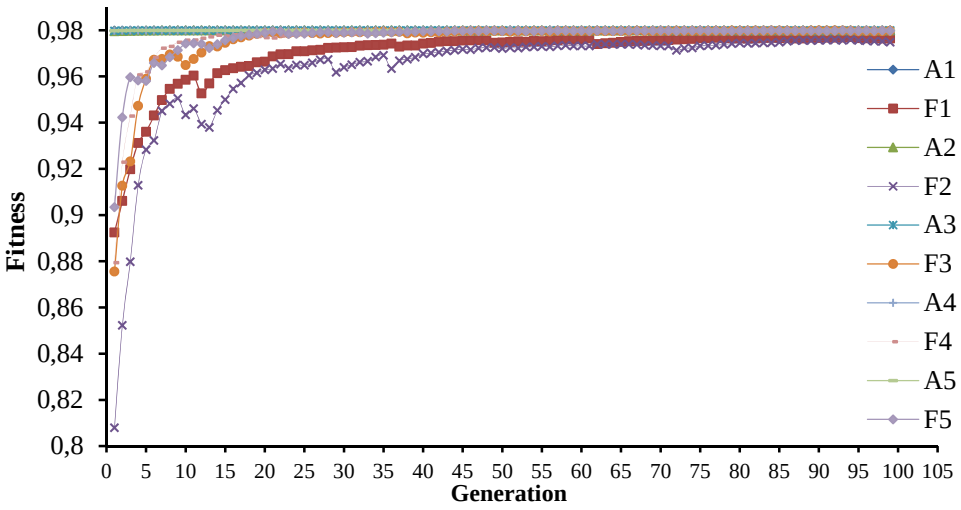

Figure 4 Results of optimization process using EMAC algorithm ("A" and "F" parameters are corresponding to Average and Fitness respectively).

Table 5 Comparison of the optimal sensor locations of the MAC and EMAC algorithms

Sensor No.	1	2
MAC algorithm	1	2
EMAC algorithm	2	4

5.3 TTFD Algorithm

Due to lack of exact dynamic response on the previous presented OSP algorithms; in this research, authors introduced TTFD algorithm using time-history analysis. In this method, the results of NTA procedure are employed so that the optimal locations can be acquired exactly.

At the first, the mentioned results in the time-domain should be transformed to frequency-domain. Any signal can completely be described in time or in frequency domain. As both representations are equivalent, it is possible to transform them to each other. This is done by the so-called Fourier Transformation (Equation (3)) and the Inverse Fourier Transformation (Equation (4)), respectively:

$$U(j\omega) = \int_{-\infty}^{+\infty} u(t).\, e^{-j\omega.\, t}\, dt \tag{3}$$

$$u(t) = \frac{1}{2\pi} \int_{-\infty}^{+\infty} U(j\omega).\, e^{j\omega.\, t}\, d\omega \tag{4}$$

After domain transformation, the periods obtained corresponding to Displacement-Time record of NTA. In following the minimum and maximum periods of the modal analysis (Table 4) were compared with the obtained periods by NTA procedure and so the maximum NTA displacements were corresponded to maximum modal responses. Figures 5 and 6 illustrate the Fourier Amplitude-Frequency diagram for far-field and near-field earthquakes respectively.

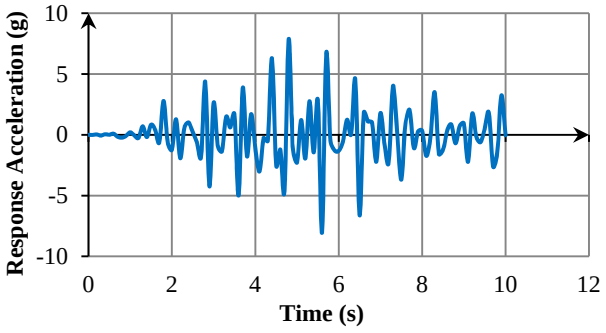

Figure 5(a) Response Acceleration-Time diagram of Chi-Chi Earthquake (1999)

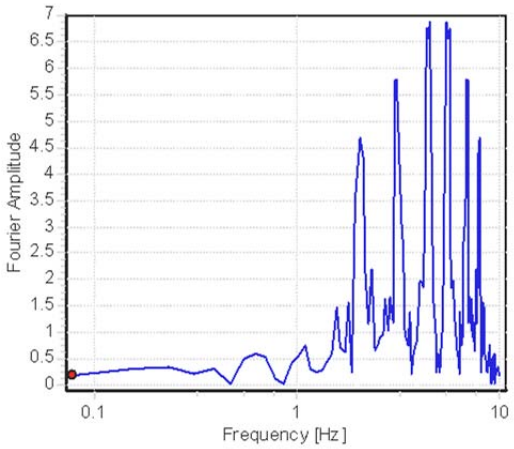

Figure 5(b) Time-Frequency domain transformation of Chi-Chi Earthquake (1999)

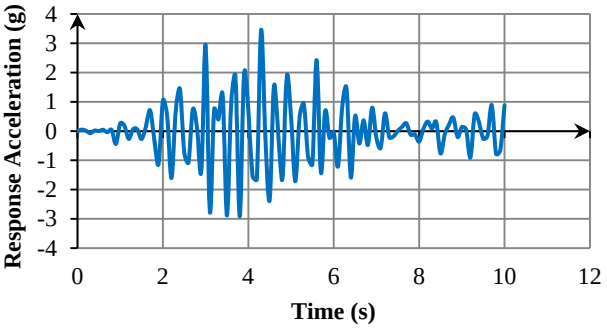

Figure 6(a) Response Acceleration-Time diagram of Northridge Earthquake (1994)

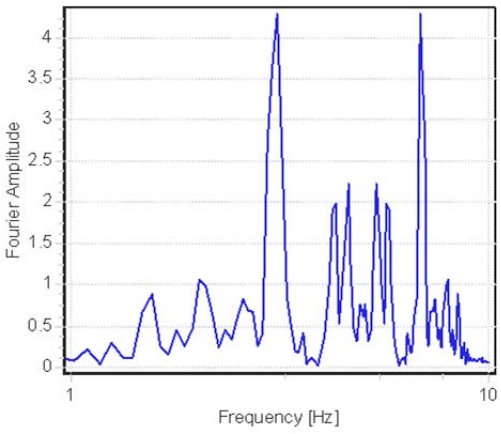

Figure 6(b) Time-Frequency domain transformation of Northridge Earthquake (1994)

The Complete Quadratic Combination (CQC) method was utilized as a well known modal combination technique in this paper but after Time-Frequency transformation authors replaced the equivalent values of NTA with the modal analysis results. Hence, all of the required parameters values in the CQC such as maximum modal responses in the *n*th and mth modes, rigid response coefficient etc were replaced with NTA transformed and equivalent results. According to Iranian seismic code [34] and also ASCE code [35], since maximum modal responses do not occur for different modes in an earthquake simultaneously therefore, it should estimate maximum modal responses in different members of structure via a statistical method. The mentioned statistical method should be as indicated by the maximum displacements of different modes and it should include the effects of probable interactions between different displacements close together that are derived from different modes. The peak value of the total response U is estimated by combining the peak modal response of individual modes using modified double sum equation; this is given by [36]:

$$U^2 = \sum_{n=1}^{N} {U_n}^2 + 2\sum_{n=1}^{N-1}\sum_{m=n+1}^{N} \rho_{nm} U_n U_m \tag{5}$$

where, U_n is the maximum modal response in the *n*th mode, and ρ_{nm} is the modified correlation factor defined as:

$$\rho_{nm} = \alpha_n \alpha_m + [(1 - {\alpha_n}^2)\,(1 - {\alpha_m}^2)]^{\frac{1}{2}}\,\rho_{nm} \tag{6}$$

where, α_n is the rigid response coefficient in the nth mode and ρ_{nm} is the correlation coefficient of the damped periodic part of modal responses, given by the well known CQC rule. For damped periodic modes, α = 0, and modified double sum equation reduces to CQC and for ρ_{nm} = 0, modified double sum method reduces this to the Square Root of Sum of Squares (SRSS). Equations (5) and (6) include the effect of rigid response of high frequency modes in the modified correlation coefficient ρ_{nm}. The rigid response coefficient α_n is defined as [36]:

$$\alpha_n = -\frac{\int_0^{t_d} \ddot{X}_n(t)\ddot{u}_g(t)dt}{t_d {\sigma_n}^{\ddot{X}} \sigma^{\ddot{u}_g}} \tag{7}$$

Where $\ddot{X}_n(t)$ is the acceleration response, ${\sigma_n}^{\ddot{X}}$ and $\sigma^{\ddot{u}_g}$ are the standard deviations of $\ddot{X}_n(t)$ and $\ddot{u}_g(t)$ respectively and t_d is the duration of responses. The modal responses, having a frequency less than rigid frequency also have a rigid content and the value of α gradually reduces from one to zero from a key frequency f_2 to another key frequency f_1 [36]. The key frequency f_2 is the lowest frequency at which the rigid response coefficient becomes 1 and the key frequency f_1 the highest frequency at which the rigid response coefficient becomes zero. An approximate equation for α_n can be represented by a straight line between the two key frequencies f_1 and f_2 on a semi logarithmic graph, this is given by [36]:

$$\alpha_n = \frac{\ln\frac{f_n}{f_1}}{\ln\frac{f_2}{f_1}} \qquad 0 \le \alpha_n \le 1 \tag{8}$$

where f_n is the modal frequency (Hz) and the key frequencies f_1 and f_2 can be expressed as,

$$f_1 = \frac{S_{A\ max}}{2\pi S_{V\ max}} \tag{9}$$

$$f_2 = \frac{(f_1 + 2f^r)}{3} \tag{10}$$

where $S_{A\ max}$ = maximum spectral acceleration, $S_{V\ max}$ = maximum spectral velocity and f^r = rigid frequency.

Now the optimization procedure can be performed by GA. In this study, the number of variables is equal to 3 and also 9 constraints have been considered. The height of braced building has been divided into 4 ranges. It should be implied that the height of the structure is 12.0 meters. So, the length of each range was found to be 3.0 meters. At the first, ρ_{nm} was calculated then the square of total response U^2 was computed using ρ_{nm}, U_n and U_m parameters. Each of the variations should be less than maximum modal response corresponding to that mode in the each range. Equation (5) was employed as Fitness function in this framework. This function was maximized by the GA system in the process of evolutionary optimization. When performing the OSP method via GA technique, certain parameters are required such as; constraints, Fitness function, population, generation, crossover method, mutation rate etc. Each of these runs started with a random initial population that was uniformly distributed within the same range. Figure 7, clearly shows that the best fitness values tend to a constant quicker along as the number of generations increases despite many fluctuations occurring that are caused by the genetic operators of crossover and mutation's search processes. Finally after obtaining U^2 values via optimization process, interpolation carried out in each range considering the initial results of the square of total response so acquired the optimal locations.

According to this optimization method and considering GA results, the most proper locations for layout of smart sensors in the building have been presented as the final results in Tables 6 and 7.

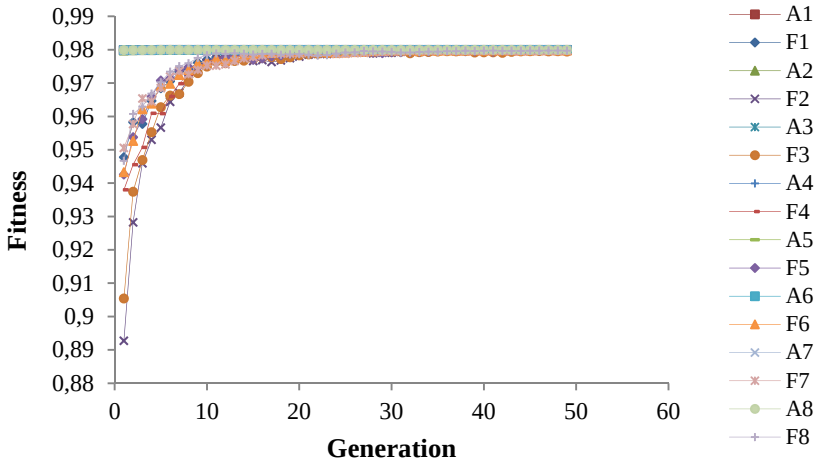

Figure 7 Results of optimization process in all of stages, evolution of the best function value performance of optimized sensor layout as compared to stages of 1 to 4 ("A" and "F" parameters are corresponding to Average and Fitness respectively).

Table 6 Details of optimization by GA in each 4 stages using a far-field earthquake

Stage	1 (0-3.0 m)	2 (3.01-6.0 m)	3 (6.01-9.0 m)	4 (9.01-12.0 m)
X direction (m)	2.17	4.48	8.06	11.14
Y direction (m)	2.04	4.11	7.65	10.54
Z direction (m)	1.68	3.96	7.23	10.28

Table 7 Details of optimization by GA in each 4 stages using a near-field earthquake

Stage	1 (0-3.0 m)	2 (3.01-6.0 m)	3 (6.01-9.0 m)	4 (9.01-12.0 m)
X direction (m)	2.49	4.79	8.52	11.46
Y direction (m)	2.31	4.46	8.31	11.13
Z direction (m)	2.14	4.17	8.02	10.89

6. Conclusions

Researches show that application of health monitoring can detect weak points of structure and it can help prevent possible damages that may occur in the future, it also plays a key role on improving the structural performance. In this paper, three reliable methods for OSP of the LSF building, based on modal and time-history analyses result, for the evaluation of objective function have been demonstrated. Real coded elitist genetic algorithms with uniform parent centric crossover operators and mutation operator have been developed and used for the implementation of the optimal placement.

In this research, MAC, EMAC and TTFD methods were investigated for OSP procedure. MAC algorithm is a common method in this field whereas EMAC is a new algorithm that has been improved MAC which both of them utilizes the free vibration analysis results. Furthermore, a novel approach was proposed by authors for OSP which was adopted TTFD algorithm. This novel approach uses time-history analysis results as an exact seismic response despite the MAC and EMAC algorithms which utilize modal analysis results. Therefore, for the health monitoring of a LSF structure, layouts of smart sensors in the mentioned points will be used to reveal the structural condition with the appropriate layouts. These will be derived from numerical methods. Once the layout of smart sensors are placed in the mentioned areas of building a safe method for health monitoring of different structures can be implemented.

References

[1] Xu, L. and Tangorra, F. M. 2007. “Experimental investigation of lightweight residential floors supported by cold-formed steel C-shape joists”, Journal of Constructional Steel Research, 63: 422–435.

[2] Al-Kharat, M. and Rogers, C. A. 2007. “Inelastic performance of cold-formed steel strap braced walls”, Journal of Constructional Steel Research 63: 460–474.

[3] Dubina, Dan. 2008. “Behavior and performance of cold-formed steel-framed houses under seismic action”, Journal of Constructional Steel Research, 64: 896–913.

[4] Moghimi, H. and Ronagh, H. R. 2009. “Performance of light-gauge cold-formed steel strap-braced stud walls subjected to cyclic loading”, Engineering Structures, 31: 69-83.

[5] Duan, H., Li, S. and Liu, Y. 2011. "A Nonlinear Two-stage Damage Identification Method for Steel Frames", International Journal of Advancements in Computing Technology, 3(4): 109-120.

[6] Nguyen, V. H. and Golinval, J. C. 2010. “Damage localization in linear-form structures based on sensitivity investigation for principal component analysis”, Journal of Sound and Vibration, 329(21): 4550-4566.

[7] Li, X. Y. and Law, S. S. 2010. “Adaptive regularization for damage detection based on nonlinear model updating”, Mechanical Systems and Signal Processing, 24(6): 1646-1664.

[8] Weber, B., Paultre, P. and Proulx, J. 2009. “Consistent regularization of nonlinear model updating for damage identification”, Mechanical Systems and Signal Processing, 23(6): 1965-1985.

[9] Yuan, X. D. and Gao, C. and Gao, S. X. 2007. “A numerical simulation for influence of measurement mode quantity on structural damage identification”, Engineering Mechanics, 24(1): 75-78.

[10] Jong, J. L. and Chung, B. Y. 2006. “Damage diagnosis of steel girder bridges using ambient vibration data”, Engineering Structures, 28(6): 912-925.

[11] Bakhary, N., Hao, H. and Deeks, A. J. 2007. “Damage detection using artificial neural network with consideration of uncertainties”, Engineering Structures, 29(11): 2806-2815.
[12] Ajdari, J. 2010. “Parallel Implementation of 2D Haar and Daubechies D4 Transform in Mesh Architecture”, IJIIP, 1(2): 55-64.
[13] Sadkhan, S. B. and Abbas, N. A. 2009. “Proposed Simulation of Modulation Identification Based On Wavelet Transform”, IJACT, 1(1): 78-84.
[14] Gao, Y., Spencer, J. B. and Ruiz, S. M. 2006. “Distributed computing strategy for structural health monitoring”, Structural Control and Health Monitoring, 13(1): 488-507.
[15] Ji, X. D., Qian, J. R. and Xu, L. H. 2007. “An experiment on localization of a two-story steel braced frame model structure”, Engineering Mechanics, 24(1): 62-66.
[16] Hemez, F. M. and Farhat, C. 1994. "An energy based optimum sensor placement criterion and its application to structure damage detection", Proceedings of the 12th Conference on International Modal Analysis (Honolulu,HI: Society of Experimental Mechanics) pp 1568–75.
[17] Miller, R. E. 1998. "Optimal sensor placement via Gaussian quadrature", Applied Mathematics and Computing, 97: 71–97.
[18] Hiramoto, K., Doki, H. and Obinata, G. 2000. "Optimal sensor/actuator placement for active vibration control using explicit solution of algebraic Riccati equation", journal of Sound and Vibration, 229: 1057–75.
[19] Wouwer, A. V., Point, N., Porteman, S. and Remy, M. 2000. "An approach to the selection of optimal sensor locations in distributed parameter systems", Journal of Process Control, 10: 291–300.
[20] Worden, K. and Burrows, A. P. 2001. "Optimal sensor placement for fault detection", Engineering Structures, 23: 885–901.
[21] Cobb, R. G. and Liebst, B. S. 1997. "Sensor placement and structural damage identification from minimal sensor information", AIAA Journal, 35: 369–74.
[22] Shi, Z. Y., Law, S. S. and Zhang, L. M. 2000. "Optimum sensor placement for structural damage detection", Journal of Engineering Mechanics, 126: 1173–9.
[23] Cruz, A., Vélez, W. and Thomson, P. 2010. "Optimal sensor placement for modal identification of structures using genetic algorithms—a case study: the Olympic stadium in Cali, Colombia", Annals of Operations Research, 181: 769–781.
[24] Yi, T. H., Li, H. N. and Gu, M. 2011. "Optimal sensor placement for health monitoring of high-rise structure based on genetic algorithm", Journal of Mathematical Problems in Engineering, Volume 11, Article ID 395101, 12 pages.
[25] http://peer.berkeley.edu
[26] Goldberg, D. E. 1989. "Genetic Algorithms in Search, Optimization and Machine Learning", Addison-Wesley Pub. Co., Reading, Mass., xiii, 412 p. pp.
[27] Tongpadungrod, P., Rhys, T. D. L. and Brett, P. N. 2003. "An approach to optimise the critical sensor locations in one-dimensional novel distributive tactile surface to maximize performance", Sensors Actuators, A., 105: 47–54.
[28] Yan, Y. J. and Yam, L. H. 2002. "Optimal design of number and locations of actuators in active vibration control of a space truss", Smart Materials and Structures, 11: 496–503.
[29] Ponslet, E. R. and Eldred, M. S. 1996. "Discrete optimization of isolator locations for vibration isolation systems", Proceedings of the 6th AIAA NASA, and ISSMO Symposia on Multi-Disciplinary Analysis and Optimization., Technical Papers (Bellevue, WA). part II .pp. 1703–16.
[30] Huang, W. P. Liu, J. and Li, H. J. 2005. “Optimal sensor placement based on genetic algorithms”, Engineering Mechanics, 22(1): 113-117.
[31] Guo, H. Y., Zhang, L., Zhang, L. L. and Zhou, J. X. 2004. "Optimal placement of sensors for structural health monitoring using improved genetic algorithms", Smart Materials and Structures, 13: 528–534.
[32] Dong, C. 1998. “Generalized genetic algorithm”, Exploration of Nature, 63(17): 33-37.
[33] Li, D. 2011. "Sensor Placement Methods and Evaluation Criteria in Structural Health Monitoring", Universität Siegen, M. S. Thesis.
[34] Iranian code of practice for seismic resistant design of buildings. 2005. Standard no. 2800, Iranian building codes and standards, Building and Housing research center, Iran.
[35] ASCE standard code. 2005. "Minimum design loads for buildings and other structures". ASCE, USA.
[36] Gupta, A. K., Hassan, T. and Gupta, A. 1996. "Correlation coefficients for modal response combination of non-classically damped systems", Nuclear Engineering and Design, 165: 67–80.
[37] Cold-Formed Steel Design Manual and Specification Bundle, 2010. AISI, USA.